located near Monte Verde, thought to be the oldest archaeological site in the Americas[18]. Remains interpreted as partially burned plant and animal artefacts in association with hearths have been cited as evidence for the presence of humans and their use of fire between ~12.5 and 12 ^{14}C kyr BP. Possibly, the high climate variability between ~11.2 and 9.9 ^{14}C kyr BP afforded the conditions that allowed humans to set small-scale fires that altered the vegetation near the Huelmo and Lago Condorito sites.

Our data suggest that climate approaching modern conditions prevailed in the Chilean Lake District between ~13 and 12.2 ^{14}C kyr BP. This was followed by a general reversal in trend with cooling events at ~12.2 and ~11.4 ^{14}C kyr BP, and then by subsequent warming at 9.8 ^{14}C kyr BP. The total temperature depression between ~11.4 and 9.8 ^{14}C kyr BP was relatively minor ($\leq 3\,^\circ$C), as indicated by the persistence of rainforest vegetation. The timing, direction, and relative magnitude of these events matches the late-glacial record from nearby Lago Mascardi[19] (Fig. 1), which indicates retreat of the Monte Tronador ice cap between 13 and 12.4 ^{14}C kyr BP, a reversal starting at ~12.4 ^{14}C kyr BP and culminating with glacial readvance between 11.4 and 10.2 ^{14}C kyr BP. These records from the Andean region of mid-latitude South America show a notable resemblance in timing and structure to palaeoclimate fluctuations recorded in Europe and Greenland. In contrast, Bennett et al.[4] found no palynological evidence for climate change during late-glacial time in the Chilean channels (45°–47° S). If this interpretation is correct, their results would imply that: (1) a major climate boundary existed between 42° and 45° S during late-glacial time; or (2) late-glacial climate changes did not reach a critical threshold to trigger discernible vegetation changes in palynological records, and thus the impoverished late-glacial flora of the Chilean channels was insensitive to the magnitude of late-glacial cooling; and/or (3) plant succession, soil development, and migration from glacial refugia were the dominant factors controlling vegetation change in this newly deglaciated region during the critical time period.

Our results suggest that mid-latitude climate in the Southern Hemisphere changed in unison with the North Atlantic region between ~13 and 10 ^{14}C kyr BP. This is in contrast with the palaeoclimate signal derived from sediment cores in the South Atlantic Ocean[20] and ice cores from interior Antarctica[21], where the pattern of climate change is opposite to that found in the Chilean Lake District between ~13 and 10 ^{14}C kyr BP. Determining the representativeness of these opposing results on a hemispheric scale has important implications for understanding the climate mechanisms operative during ice ages, because one set of data supports an in-phase interhemispheric linkage in the atmosphere[2,22,23], whereas the other favours an out-of-phase relationship via a bipolar see-saw in deep ocean circulation[24]. The solution could well be that synchronous climate changes, propagated in the atmosphere over much of the planet, were counteracted in Antarctica by a bipolar see-saw of thermohaline circulation, whose effects in the Southern Hemisphere were confined to the high southern latitudes. □

1. Denton, G. H. et al. Interhemispheric linkage of paleoclimate during the last glaciation. Geogr. Ann. A 81, 107–155 (1999).
2. Lowell, T. V. et al. Interhemispheric correlation of Late Pleistocene glacial events. Science 269, 1541–1549 (1995).
3. Zhou, M. & Heusser, C. J. Late-glacial palynology of the Myrtaceae of Chile. Rev. Palaeobot. Palynol. 91, 283–315 (1996).
4. Bennett, K. D., Haberle, S. G. & Lumley, S. H. The last glacial-Holocene transition in Southern Chile. Science 290, 325–328 (2000).
5. Denton, G. H. & Hendy, C. H. The age of the Waiho Loop glacial event. Science 271, 668–670 (1995).
6. Denton, G. H. & Hendy, C. H. Younger Dryas age advance of Franz Josef Glacier in the Southern Alps of New Zealand. Science 264, 1434–1437 (1994).
7. Singer, C., Shulmeister, J. & McLea, B. Evidence against a significant Younger Dryas cooling event in New Zealand. Science 281, 812–814 (1998).
8. Newnham, R. M. & Lowe, D. J. Fine-resolution pollen record of late-glacial climate reversal from New Zealand. Geology 28, 759–762 (2000).
9. Björk, S. et al. An event stratigraphy for the Last Termination in the North Atlantic region based on the Greenland ice-core record: a proposal by the INTIMATE group. J. Quat. Sci. 13, 281–292 (1998).
10. Villagrán, C. Vegetatiosgeschichtliche und pflanzensoziologische Untersuchungen im Vicente Perez Rosales National park (Chile). Diss. Bot. 54, 1–165 (1980).
11. Páez, M. M., Villagrán, C. & Carrillo, R. Modelo de la dispersión polínica actual en la región templada chileno-argentina de Sudamérica y su relación con el clima y la vegetación. Rev. Chil. Hist. Nat. 67, 417–434 (1994).
12. Mercer, J. H. Glacial history of southernmost South America. Quat. Res. 6, 125–166 (1976).
13. Mercer, J. H. Chilean glacial chronology 20,000 to 11,000 carbon-14 years ago: some global comparisons. Science 172, 1118–1120 (1972).
14. Porter, S. C. Pleistocene glaciation in the southern lake district of Chile. Quat. Res. 16, 263–292 (1981).
15. Lusk, C. H. Gradient analysis and disturbance history of temperate forests of the coast range summit plateau, Valdivia, Chile. Rev. Chil. Hist. Nat. 69, 401–411 (1996).
16. Lusk, C. H. Long-lived light-demanding emergents in southern temperate forests: the case of Weinmannia trichosperma (Cunoniaceae) in southern Chile. Plant Ecol. 140, 111–115 (1999).
17. Ramírez, C. in Monte Verde, a Late Pleistocene Settlement in Chile Vol. I, Paleoenvironment and Site Context 53–87 (Smithsonian Institution Press, Washington, 1989).
18. Dillehay, T. Monte Verde, a Late Pleistocene Settlement in Chile. Vol. II, The Archaeological Context and Interpretation (ed. Gould, R. A.) (Smithsonian Institution Press, Washington, 1997).
19. Ariztegui, D., Bianchi, M. M., Masaferro, J., Lafargue, E. & Niessen, F. Interhemispheric synchrony of late-glacial climatic instability as recorded in proglacial Lake Mascardi, Argentina. J. Quat. Sci. 12, 333–338 (1997).
20. Charles, C. D., Lynch-Stieglitz, J., Ninnemann, U. S. & Fairbanks, R. G. Climate connections between the hemispheres revealed by deep sea sediment core/ice core correlations. Earth Planet. Sci. Lett. 142, 19–27 (1996).
21. Sowers, T. & Bender, M. Climate records covering the last deglaciation. Science 269, 210–214 (1995).
22. Broecker, W. S. & Denton, G. H. The role of ocean-atmosphere reorganizations in glacial cycles. Quat. Sci. Rev. 9, 305–341 (1989).
23. Broecker, W. S. Massive iceberg discharges as triggers for global climate change. Nature 972, 421–424 (1994).
24. Broecker, W. S. Paleocean circulation during the last deglaciation: A bipolar seesaw? Paleoceanography 13, 119–121 (1998).

Evidence of recent volcanic activity on the ultraslow-spreading Gakkel ridge

M. H. Edwards*, G. J. Kurras†, M. Tolstoy‡, D. R. Bohnenstiehl‡, B. J. Coakley§ & J. R. Cochran‡

* Hawaii Institute of Geophysics and Planetology, POST 815; † Department of Geology and Geophysics, POST 842A, School of Ocean and Earth Science and Technology, University of Hawaii at Manoa, 1680 East-West Road, Honolulu, Hawaii 96822, USA
‡ Lamont-Doherty Earth Observatory, Columbia University, 61 Route 9W, Palisades, New York 10964, USA
§ Department of Geology, Tulane University, New Orleans, Louisiana 70118, USA

Seafloor spreading is accommodated by volcanic and tectonic processes along the global mid-ocean ridge system. As spreading rate decreases the influence of volcanism also decreases[1–4], and it is unknown whether significant volcanism occurs at all at ultraslow spreading rates ($<1.5\,$cm yr^{-1})? Here we present three-dimensional sonar maps of the Gakkel ridge, Earth's slowest-spreading mid-ocean ridge, located in the Arctic basin under the Arctic Ocean ice canopy. We acquired this data using hull-mounted sonars attached to a nuclear-powered submarine, the USS Hawkbill. Sidescan data for the ultraslow-spreading

(~1.0 cm yr^{-1}) eastern Gakkel ridge depict two young volcanoes covering approximately 720 km^2 of an otherwise heavily sedimented axial valley. The western volcano coincides with the average location of epicentres for more than 250 teleseismic events detected[5,26] in 1999, suggesting that an axial eruption was imaged shortly after its occurrence. These findings demonstrate that eruptions along the ultraslow-spreading Gakkel ridge are focused at discrete locations and appear to be more voluminous and occur more frequently than was previously thought.

The Arctic basin is the last of Earth's oceanic frontiers. Permanent pack ice covers the Arctic Ocean, restricting the free motion of surface ships, making it impossible to map the sea floor comprehensively. The ice canopy impedes the use of satellite altimetry data to derive the predicted bathymetry models that now exist for every other ocean[6,7]. Nuclear submarines are ideal for Arctic research because they operate beneath the pack ice and are thus independent of surface conditions. In 1995 the US Navy and National Science Foundation cooperatively developed the Science Ice Exercises (SCICEX), a five-year programme supported by nuclear-powered Sturgeon-class submarines to study the ice canopy, oceanography, biology and geology of the Arctic basin. For SCICEX-98 and SCICEX-99 the US Navy's submarine USS *Hawkbill* was equipped with the Seafloor Characterization and Mapping Pods (SCAMP), a geophysical mapping system built to create the first three-dimensional maps of the Arctic sea floor. SCAMP instrumentation includes a 12-kHz Sidescan Swath Bathymetric Sonar (SSBS), a swept frequency (2.75 kHz to 6.75 kHz) High-Resolution Sub-bottom Profiler (HRSP), a BGM-3 gravimeter and the Data Acquisition and Quality Control System (DAQCS)[8]. We used the Submarine Inertial Navigation system to navigate under the ice, supplemented by occasional fixes from the Global Positioning Satellite network when the USS *Hawkbill* surfaced. Our relative positional accuracy was better than 3 km.

The SCICEX-99 survey of Gakkel ridge was carried out at an operating depth of 225 m and a speed of 16 knots. The average usable swath width for bathymetry data is 10 km; the average swath width for sidescan data is 16 km. Typical sub-bottom penetration in sedimented areas is 100 m. SCICEX-98 and SCICEX-99 data provide approximately 100% bathymetric and sidescan coverage for the western Gakkel ridge rift valley and flanks out to 50 km on both sides of the ridge axis. Full spreading rates range from 1.33 cm yr^{-1} to 1.15 cm yr^{-1} (ref. 9) at the ends of this region (Fig. 1). During SCICEX-99 a reconnaissance survey of the eastern Gakkel ridge extended coverage of the axial zone out to 1.0 cm yr^{-1} full-spreading rate[9].

One goal of the SCICEX surveys was to resolve a debate regarding the nature of volcanism at the ultraslow-spreading Gakkel ridge. The presence of lineated magnetic anomalies[10,11] over the entire ridge suggests that seafloor volcanism occurs. Three bathymetric profiles across the axis of Gakkel ridge near 15° E depict a central high with 200 m relief[12] on the axial valley floor that may be a constructional ridge analogous to those observed on the slow-spreading Mid-Atlantic Ridge[13,14]. However, theoretical modelling predicts that melt production should be diminished, or even inhibited, at spreading rates less than 1.5 cm yr^{-1} (refs 1–4). Analysis of SCICEX-96 gravity data suggests that the Gakkel ridge crust is anomalously thin[15], supporting a hypothesis of diminished volcanism. The paucity of high-resolution bathymetry and sidescan data for Gakkel ridge has prevented unequivocal identification of any volcanic features until now.

SCICEX-99 sidescan and bathymetry data for the reconnaissance survey of the eastern Gakkel ridge show two amorphously shaped
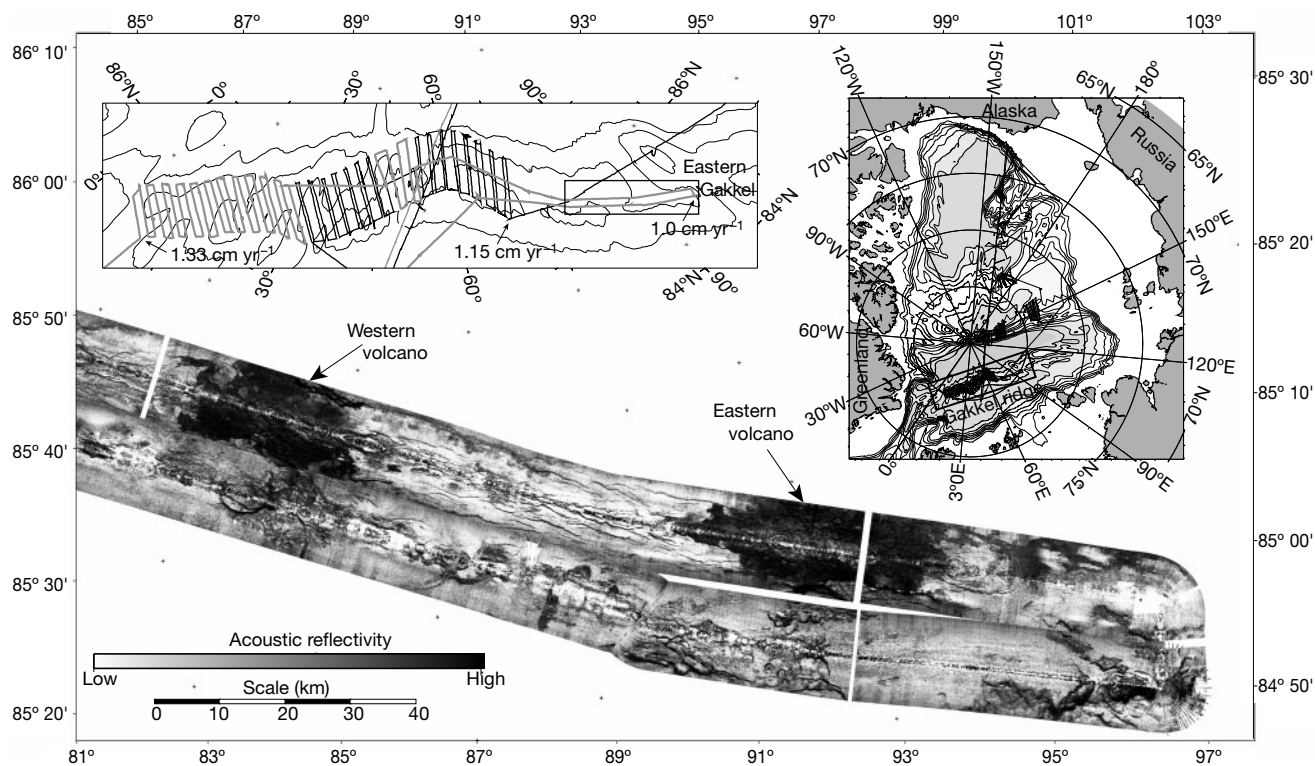
Figure 1 SCAMP sidescan data for the eastern Gakkel ridge. Two areas with high acoustic return strength, labelled the western volcano and eastern volcano, are probably younger than the weakly reflective terrain, presumably covered with thicker sediments, that surrounds them. Upper right inset, location map showing the Gakkel ridge survey within the Arctic basin. Bathymetric contour interval is 500 m; deeper regions are indicated by darker shades of grey. SCICEX-99 tracklines are shown in black. Upper left inset, detail of the SCICEX-98 (black) and SCICEX-99 (grey) tracklines for the Gakkel ridge surveys. Full spreading rates are indicated in three locations. The rectangle on the right side of the map shows the location of the sidescan data displayed below the insets.

areas with highly reflective acoustic character (Fig. 1) that are also topographic highs with 1,000 and 500 m relief, respectively (Figs 2 and 3). The sidescan data show long, sinuous channels of very reflective (dark grey) terrain, adjacent to and occasionally surrounding less reflective (light grey) terrain. The regions with lower acoustic reflectivity are interpreted to have thick sediment cover; the attenuation of sound waves in sediments reduces the strength of acoustic echoes[16]. Average sedimentation rates for the eastern Arctic are estimated to be 1–3 cm kyr^{-1} (ref. 17), increasing as Gakkel ridge approaches the Laptev shelf. Given the 12.5-cm operational wavelength of the SSBS and the estimated sedimentation rate, it would take thousands of years to create sediment cover thick enough to attenuate the strength of the acoustic return significantly. We thus interpreted regions of low acoustic return to be older than strongly reflective regions.

Portions of the strongly reflective regions in the SCICEX-99 sidescan data abut lineaments, consistent with the ponding of lava against fault scarps (Fig. 2). Terminations of acoustically reflective terrain in regions devoid of lineaments have shapes characteristic of lava flow fronts or 'toes' (Fig. 3). The flow toes are radially distributed around the topographic highs. The morphology of the

strongly reflective regions is consistent with submarine volcanic flows mapped at other mid-ocean ridges by acoustic and optical systems[18–20]. The acoustic character of the highly reflective Gakkel ridge terrain is very similar to a lava field at 8° S on the East Pacific Rise that was first detected because of its strong acoustic reflectivity[18] and was subsequently shown to contain fresh, glassy basalts[21]. The two acoustically reflective regions are thus probably volcanoes that are largely devoid of sediment cover, and therefore erupted recently. The presence of these two young volcanoes, covering approximately 20% of the 3,750 km^2 surveyed along this portion of the eastern Gakkel ridge, proves that significant volcanism occurs at ultraslow spreading rates.

The sidescan data reveal that both volcanoes are cut by lineations interpreted to be faults formed by tectonic processes that occurred subsequent to volcanic emplacement. The western volcano (Fig. 3) is significantly less faulted than the eastern volcano (Fig. 2), suggesting that lava on the western volcano experienced less post-emplacement tectonism and is therefore younger. The few faults evident on the western volcano are located near the southern flank of the topographic high. Two of these faults traverse abrupt changes in acoustic reflectivity; these light/dark contacts indicate significant
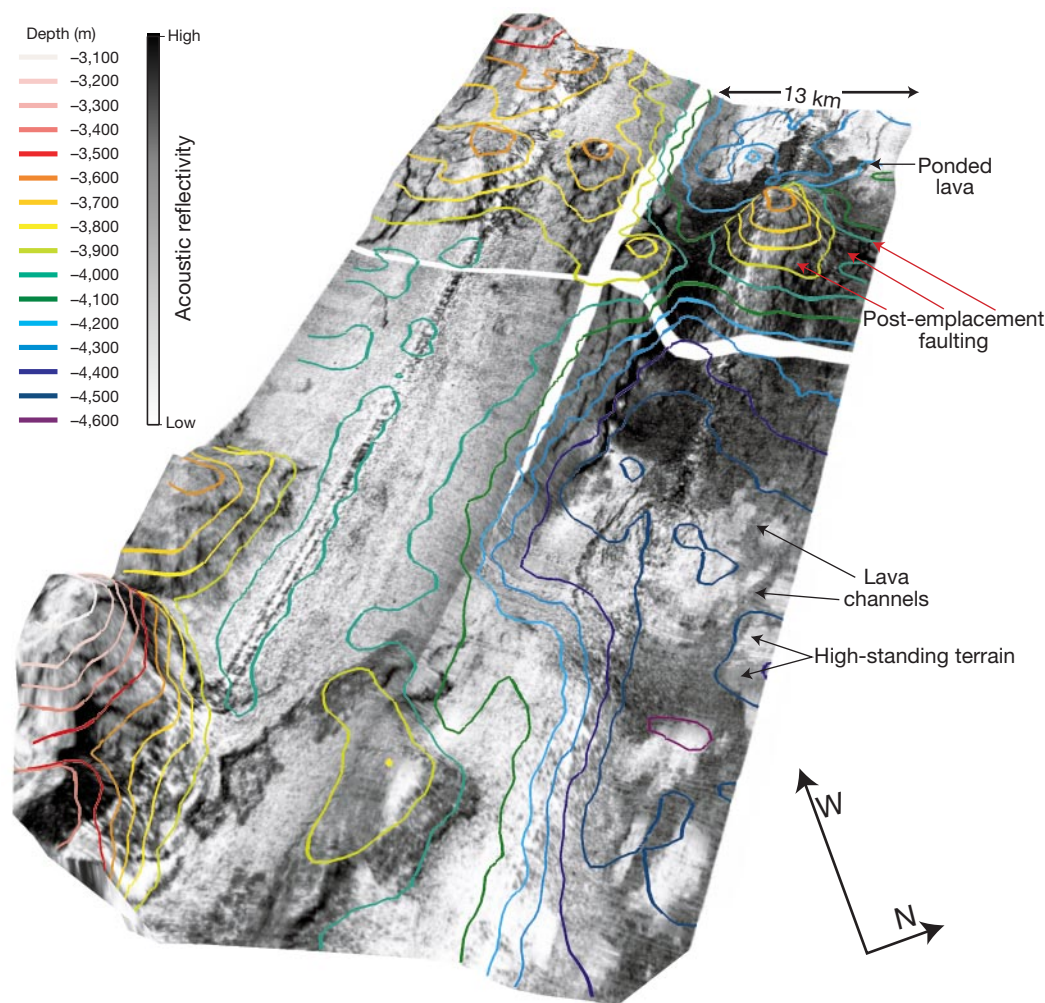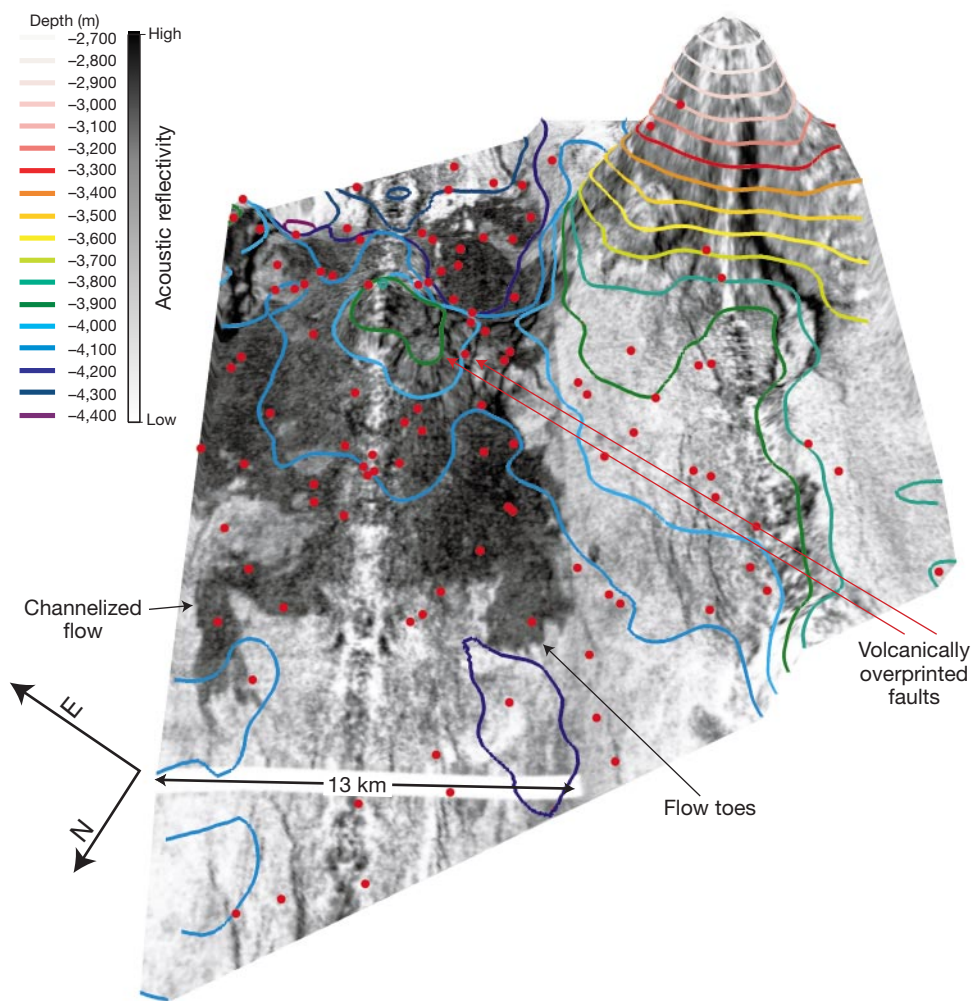

Figure 2 Three-dimensional view of the eastern volcano looking from east to west. In this image sidescan data are overlaid on a digital terrain model derived from SCAMP bathymetry. Colour-coded contours indicate depth. The region of highly reflective terrain located near the upper right corner of the data is approximately centred about a 1,000-m topographic high. To the west and east of the topographic high, sinuous channels of reflective terrain spill downslope. Where these channels adjoin lineations or higher-elevation terrain they abruptly terminate or flow around features. This morphology is consistent with submarine lava flows observed on other mid-ocean ridges. The reflective terrain on the eastern volcano is laced with WNW–ESE trending lineations. These lineations are interpreted to be faults caused by tectonism that occurred after the emplacement of the reflective volcanic terrain. See Fig. 1 for the location of the eastern volcano.

differences in the amount of sediment cover. We interpret them to represent a boundary between lava flows of different ages. The presence of faults having sufficient vertical offset to be imaged by SCAMP indicates that the southern flank of the western volcano did not erupt recently. Assuming reasonable geological slip rates of a few mm yr^{-1} (refs 22, 23), faults of sufficient size to be imaged by SCAMP in ~4,000 m of water depth would require hundreds to several thousands of years to develop, although collapse events can form large scarps over short time periods[24]. In contrast, the northern flank of the western volcano is remarkably devoid of lineations. In addition, all of the faults on the western volcano terminate abruptly to both the northwest and southeast. The abrupt truncation of faults on the western volcano and the absence of lineations in sidescan data for the northern flank support our hypothesis of a recent eruption that volcanically overprinted pre-existing faults. The volcanic overprinting and the presence of faults that cross-cut regions with different amounts of sediment cover lead us to conclude that the western volcano was formed by more than one eruption.

Teleseismic data for the Arctic basin corroborates the hypothesis of a recent Gakkel ridge eruption. In January 1999 global seismic networks detected the beginning of an earthquake swarm on Gakkel ridge centred near 86° N, 85° E (refs 5, 26). Seismic activity continued through September 1999 although 75% of the events took place before the end of May. On 6 May 1999, the USS *Hawkbill* passed directly over the average location of the earthquake epicentres. The average location of the epicentres corresponds to the location of the western volcano (Fig. 3). The remarkable correlation between the locations of the earthquake epicentres and the location of the strongly reflective, untectonized western volcano together with the volcanic character of the seismic record[5,26] provide evidence that lava erupted on the eastern Gakkel ridge days to months before SCAMP mapped the area. Because 12-kHz sonars can penetrate through thin sediments covering acoustically reflective lavas[25], it is possible that no eruption occurred on Gakkel ridge in 1999; however, historical global seismic records indicate that this is the only earthquake swarm detected on Gakkel ridge in about 100 years (ref. 5). SCAMP HRSP data show no evidence of sediment layering on either volcano although there is evidence of layering adjacent to both (Fig. 4). Taken together, the SCICEX and teleseismic data

Figure 3 Three-dimensional view of the western volcano looking from west to east. Data presentation is analogous to that described for Fig. 2. The dark, reflective terrain is centred about a close-contoured high having a maximum vertical relief of 500 m. As in Fig. 2, lava channels spill downslope from the volcano, ponding against fault scarps or terminating in flow toes that are characteristic of eruptive processes. Lava on the western volcano is significantly less faulted than lava on the eastern volcano (Fig. 2). The few faults evident on the southern flank of the western volcano are located on a small saddle between the western volcano and the prominent volcano to its south (right). On the saddle, these faults cut through both strongly and poorly reflective terrain indicating that at least some of the highly reflective terrain has undergone substantial tectonic modification. However, the faults abruptly terminate to west and east of the saddle, suggesting that they have been volcanically overprinted. Red circles show the locations of epicentres for the Gakkel ridge earthquake swarm that ran from January until September in 1999. See Fig. 1 for the location of the western volcano.
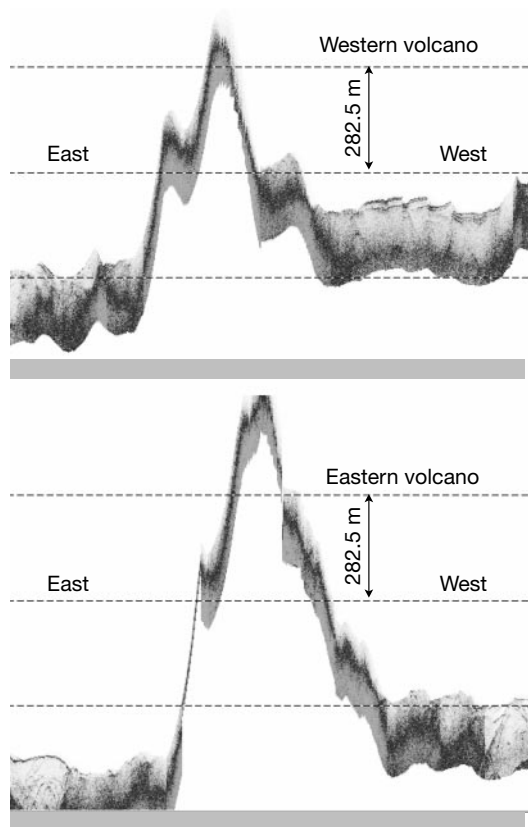
Figure 4 SCAMP sub-bottom data for the western and eastern volcanoes show no evidence of sediment layering on top of the constructs, although layers are apparent adjacent to the flanks of both highs. In these plots the *x*-axis represents time; the USS *Hawkbill* was heading from east to west when the data were collected. Vertical relief is indicated.

provide a revised model for volcanism at the ultraslow-spreading Gakkel ridge, in which voluminous, sustained eruptions focused at discrete sites may have occurred more frequently than previously thought. □

1. Chen, Y. J. Oceanic crustal thickness versus spreading rate. *Geophys. Res. Lett.* **19,** 753–756 (1992).
2. Bown, J. W. & White, R. S. Variation with spreading rate of oceanic crustal thickness and geochemistry. *Earth Planet. Sci. Lett.* **121,** 435–449 (1994).
3. Sparks, D. W., Parmentier, E. M. & Phipps Morgan, J. Three-dimensional mantle convection beneath a segmented spreading center: Implications for along-axis variations in crustal thickness and gravity. *J. Geophys. Res.* **98,** 21977–21995 (1993).
4. Reid, I. & Jackson, H. R. Oceanic spreading rate and crustal thickness. *Mar. Geophys. Res.* **5,** 165–172 (1981).
5. Müller, C. & Jokat, W. Seismic evidence for volcanic activity discovered in central Arctic. *Eos* **81,** 265–269 (2000).
6. Laxon, S. & McAdoo, D. Arctic Ocean gravity field derived from ERS-1 satellite altimetry. *Science* **265,** 621–624 (1994).
7. Smith, W. H. F. & Sandwell, D. T. Global sea floor topography from satellite altimetry and ship depth soundings. *Science* **277,** 1956–1962 (1997).
8. Chayes, D. *et al.* Swath Mapping the Arctic Ocean from US Navy submarines; installation and performance analysis of SCAMP operations during SCICEX 1998. *Eos* **79,** F854 (1998).
9. DeMets, C., Gordon, R. G., Argus, D. F. & Stein, S. Current plate motions. *Geophys. J. Int.* **101,** 425–478 (1990).
10. Vogt, P. R., Taylor, P. T., Kovacs, L. C. & Johnson, G. L. Detailed aeromagnetic investigation of the Arctic Basin. *J. Geophys. Res.* **84,** 1071–1089 (1979).
11. Coles, R. L. & Taylor, P. T. in *The Arctic Ocean Region, The Geology of North America* Vol. L, 119–132 (eds Grantz, A., Johnson, G. L. & Sweeney, J. F.) (Geological Society of America, Boulder, CO, 1990).
12. Kristoffersen, Y. The Nansen Ridge, Arctic Ocean: Some geophysical observations of the rift valley at slow spreading rate. *Tectonophysics* **89,** 161–172 (1982).
13. Ballard, R. D. & Van Andel, T. H. Morphology and tectonics of the inner rift valley at lat 36° 50′ N on the Mid-Atlantic Ridge. *Geol. Soc. Am. Bull.* **88,** 507–530 (1977).
14. Smith, D. K. & Cann, J. R. Constructing the upper crust of the Mid-Atlantic Ridge: A reinterpretation based on the Puna Ridge, Kilauea Volcano. *J. Geophys. Res.* **104,** 25379–25399 (1999).
15. Coakley, B. J. & Cochran, J. R. Gravity evidence of very thin crust at the Gakkel Ridge (Arctic Ocean). *Earth Planet. Sci. Lett.* **162,** 81–95 (1998).
16. Urick, R. J. *Principles of Underwater Sound* 136–143 (McGraw-Hill, New York, 1983).
17. Thiede, J., Clark, D. L. & Herman, Y. in *The Arctic Ocean Region: The Geology of North America* Vol. L 427–458 (eds Grantz, A., Johnson, G. L. & Sweeney, J. F.) (Geological Society of America, Boulder, CO, 1990).
18. Macdonald, K. C., Haymon, R. & Shor, A. A 220 km^2 recently erupted lava field on the East Pacific Rise near lat 8° S. *Geology* **17,** 212–216 (1989).
19. Johnson, H. P. & Helferty, M. The geological interpretation of side-scan sonar. *Rev. Geophys.* **28,** 357–380 (1990).
20. Chadwick, W. W., Embley, R. W. & Fox, C. G. Evidence for volcanic eruption on the southern Juan de Fuca ridge between 1981 and 1987. *Nature* **350,** 416–418 (1991).
21. Hall, L. S. & Sinton, J. M. Geochemical diversity of the large lava field on the flank of the East Pacific Rise at 8° 17′ S. *Earth Planet. Sci. Lett.* **142,** 241–251 (1996).
22. McAllister, E. & Cann, J. R. in *Tectonic, Hydrothermal and Geological Segmentation of Mid-Ocean Ridges* (eds MacLeod, C. J., Tyler, P. A. & Walker, C. L.) 29–48 (Geol. Soc. Spec. Pub. 188. Geological Society of America, Boulder, CO, 1996).
23. Stein, R. S., Briole, P., Ruegg, J. C., Tapponier, P. & Gasse, F. Contemporary, Holocene and Quaternary deformation of the Asal Rift, Djibouti: Implications for the mechanics of slow spreading ridges. *J. Geophys. Res.* **96,** 21789–21806 (1991).
24. Simkin, T. & Howard, K. A. Caldera collapse in the Galapagos Islands, 1968. *Science* **169,** 429–437 (1970).
25. Crane, K. *et al.* Volcanic and seismic swarm events on the Reykjanes Ridge and their similarities to events on Iceland: Results of a rapid response mission. *Mar. Geophys. Res.* **19,** 319–337 (1997).
26. Tolstoy, M., Bohnenstiehl, D. R., Edwards, M. H. & Kurras, G. J. Eruption processes at the ultra-slow spreading Gakkel Ridge. *Eos* **81,** F1346 (2000).